Tuning of Continuous-Time Filters in the Presence of Parasitic Poles

Karen A. Kozma, *Student Member, IEEE,* David A. Johns, *Member, IEEE,* and Adel S. Sedra, *Fellow, IEEE*

Abstract— **The parasitic effects and tuning limitations that nonideal integrators have on continuous-time filters are discussed. The nonideal integrator is modeled to have finite dc gain and a single nondominant pole. The performance of an adaptive tuning system on tuning a continuous-time filter with nonideal integrators is compared to the popular approach of tuning only the poles of a transfer function. Simulation results are presented showing that the adaptive tuning system significantly reduces parasitic effects.**

I. Introduction

IT IS well known that integrated continuous-time filters must be tuned in order to achieve accurate transfer-functions over time [1]. The most popular technique used for tuning continuous-time filters is the master–slave tuning method [1]–[8]. This method tunes "slave" biquad sections of a filter by first tuning the pole frequencies and quality factors of a "master" biquad and then relying on matching between corresponding elements of the master and the slave biquads. Previous work has shown that an adaptive tuning approach offers several advantages over the master–slave method [9]. In addition to tuning the poles of the transfer function, the adaptive technique tunes the zeros as well, thereby enabling a closer match to the desired transfer-function. Unlike the master–slave approach, there are no critical matching requirements between integrated elements. Also, if the filter is constructed using integrator blocks, as is the case with the filters considered in this investigation, the finite dc gains of the integrators are completely accounted for by the adaptive tuning system. Furthermore, like the master–slave method, the adaptive tuning system may be used to tune a filter without interrupting the servicing of an input signal [9].

As the operating frequency of the continuous-time filter is increased, the nonideal effects of parasitic capacitances become more pronounced, and tuning becomes more difficult. The presence of such parasitic elements, which give rise to nondominant poles in the integrators, increases the effective order of the filter by introducing parasitic poles and zeros in its transfer function without adding any extra degrees of freedom for tuning. Few tuning techniques [10] directly address the problem of dealing with parasitic effects; rather, most methods assume that the parasitic poles and zeros occur at frequencies much higher than the frequencies of interest.

Manuscript received July 31, 1992; revised December 23, 1992. This work was supported in part by Micronet and by the Natural Sciences and Engineering Research Council of Canada. This paper was recommended by Associate Editor D. J. Allstot.

The authors are with the Department of Electrical Engineering, University of Toronto, Toronto, Ontario, M5S 1A4.

IEEE Log Number 9207935.

This paper shows that the adaptive tuning method does reduce the effects of parasitic elements in the integrators. In Section II the model utilized in this investigation for the nonideal integrator is described and the resulting problems encountered in tuning the filter are discussed. Specifically, the nonideal integrator is assumed to have finite dc gain and, due to the parasitic capacitances at internal nodes, to have acquired a single nondominant pole. It is shown that the nondominant pole doubles the order of the tunable filter but does not increase the number of parameters that may be varied independently to tune the filter. In Section III, a brief review of the adaptive tuning system is given. Lastly, in Sections IV and V, simulation results are presented. Emphasis is placed on low-pass transfer-functions for use in anti-aliasing filters. It should be noted that since the adaptive tuning system tunes the impulse response of the filter, it accurately adjusts both the magnitude and phase of the transfer-function. Thus, although the filters presented in the simulations do not have flat group-delay responses, the consistent accuracy of the adaptive tuning system makes later equalization of the group-delay feasible. Although it is obvious that tuning the poles as well as the zeros would result in better transfer-function matching in the absence of parasitics, the simulation results illustrate that tuning the zeros is necessary if the parasitic effects are to be minimized. Furthermore, how tuning the zeros enables the minimization of the effects of parasitics is explained in the paper. Lastly, the simulation results also show that the type of transfer function chosen to meet required specifications affects how accurately the filter is tuned.

II. Effects of Integrator Nonidealities on Filter Tunability

As mentioned above, each integrator in the tunable filter is assumed to have finite dc gain and a single nondominant pole. In actual circuits, parasitic elements such as stray capacitances result in the integrator having multiple nondominant poles [11]. The nondominant poles are not a major concern in low-frequency applications since they would occur at frequencies much higher than the unity-gain frequency of the integrator. However, when the integrator is operated at high frequencies, the parasitic effects of the nondominant poles become significant and their effects cannot be ignored. In this investigation, the effects of multiple nondominant high-frequency poles are approximated by a single nondominant pole at a frequency comparable to the unity-gain frequency of the integrator. In order to understand how the finite dc gain and the nondominant pole affect the transfer function and limit the tunability of the filter, each is considered separately.

First, consider an integrator which has infinite dc gain but has acquired a single nondominant pole, ρ. Instead of the ideal transfer-function

$$T_{\text{int}}(s) = \frac{1}{s} \tag{1}$$

the transfer function of the integrator becomes second-order,

$$T_{\text{int}}(s) = \frac{1}{s\left(\frac{s}{\rho}+1\right)} \tag{2}$$

where ρ is the frequency of the nondominant pole, and the unity gain frequency of the integrator, ω_0 is assumed to be 1 rad/s. Fig. 1 compares the transfer functions of the ideal and nonideal integrators. As shown in Fig. 1(b) the nondominant pole, ρ, results in a sharper roll-off at high frequencies and excess phase lag at the unity-gain frequency, ω_o, of the integrator.

If each integrator in the tunable filter has the transfer function in (2), the order of the filter doubles. Specifically, let the transfer function of an Nth-order tunable filter with ideal integrators be expressed as

$$\hat{T}(s) = \hat{K}\frac{(s-\hat{z}_1)\ldots(s-\hat{z}_i)\ldots(s-\hat{z}_{N-1})}{(s-\hat{p}_1)\ldots(s-\hat{p}_i)\ldots(s-\hat{p}_N)} \tag{3}$$

where $\hat{K}$ is the tunable gain coefficient, $\hat{z}_i$ are the tunable zeros, and $\hat{p}_i$ are the tunable poles.[1] Only $N-1$ zeros are shown as the filters considered here are assumed to have at least one zero at infinity. Each tunable pole (or zero) in (3) may be represented by

$$s = \hat{\sigma} + j\hat{\omega} \tag{4}$$

where $\hat{\sigma}$ and $\hat{\omega}$ are the variable parameters of the pole (or zero). Now, if the integrators are nonideal as described in (2), each s in (3) is replaced by $s^2/\rho + s$. Thus the poles and zeros are obtained from

$$\frac{s^2}{\rho} + s = \hat{\sigma} + j\hat{\omega} \tag{5}$$

or,

$$s = -\frac{\rho}{2} \pm \frac{\rho}{2}\sqrt{1 + \frac{4}{\rho}\hat{\sigma} + j\frac{4}{\rho}\hat{\omega}}. \tag{6}$$

The above equation shows that the original pole (or zero) is mapped to a pair of poles (or zeros) which are both adjustable but are not independent as both are controlled by varying $\hat{\sigma}$ and $\hat{\omega}$. Also, the tunability of the mapped poles (or zeros) is further limited as it is assumed that the nondominant pole of the integrator, ρ, is determined by the circuit topology and is not easily controlled. Consequently, the Nth-order transfer-function in (3) becomes a $2N$th-order transfer-function

$$\hat{T}(s) = \hat{K}\frac{(s-\hat{z}_{1a})\ldots(s-\hat{z}_{ia})\ldots(s-\hat{z}_{(N-1)a})}{(s-\hat{p}_{1a})\ldots(s-\hat{p}_{ia})\ldots(s-\hat{p}_{Na})} \times \frac{(s-\hat{z}_{1b})\ldots(s-\hat{z}_{ib})\ldots(s-\hat{z}_{(N-1)b})}{(s-\hat{p}_{1b})\ldots(s-\hat{p}_{ib})\ldots(s-\hat{p}_{Nb})}. \tag{7}$$

[1] Tunable quantities are indicated by "^."

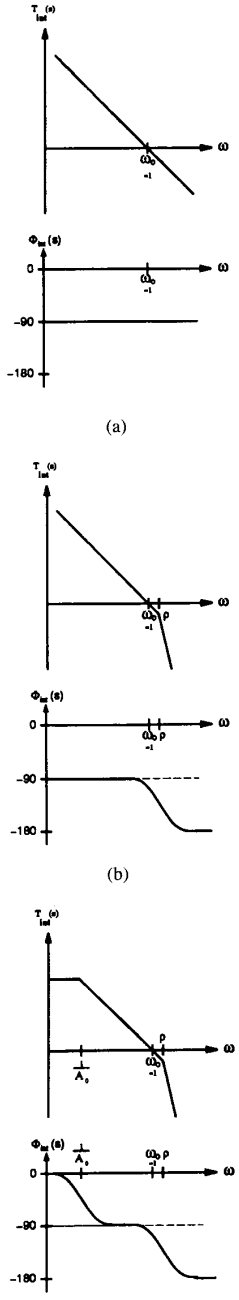

Fig. 1. Frequency responses of (a) an ideal integrator; (b) an integrator with a single nondominant pole and; (c) an integrator with a nondominant pole and finite dc gain.

Here, $\hat{p}_{ia}$ and $\hat{p}_{ib}$ denote the pair of *dependent* poles to which $\hat{p}_i$ is mapped by (6). Likewise, $\hat{z}_{ia}$ and $\hat{z}_{ib}$ represent the pair of zeros corresponding to $\hat{z}_i$. Therefore, the tuning system must adjust a $2N$th-order transfer-function which, although having twice as many variable elements as the ideal tunable filter, has no extra degrees of freedom due to the interdependence of each pair of poles (and zeros).

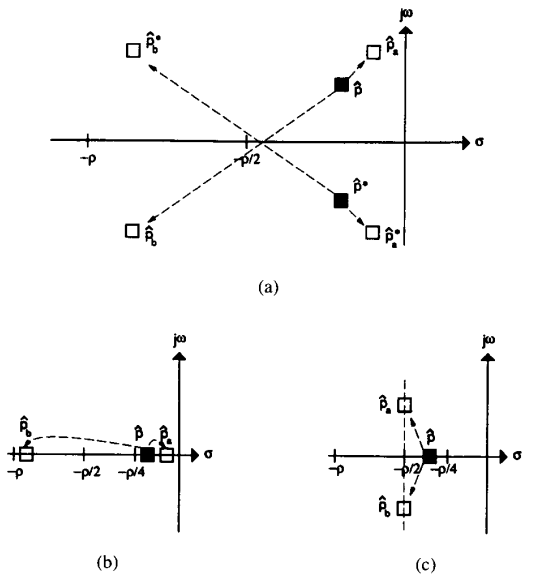

Fig. 2. Possible pole mappings due to nondominant pole in the integrator.

Using the notation of $\hat{p}$ being mapped to $\hat{p}_a$ and $\hat{p}_b$, possible pole mappings are shown in Fig. 2. For example, a pair of complex conjugate poles, $\hat{p}$ and $\hat{p}*$, are shown to be mapped to two pairs of complex conjugate poles in Fig. 2(a). The pole $\hat{p}$ is mapped to two *dependent* poles $\hat{p}_a$ and $\hat{p}_b$. Note that $\hat{p}_a$ would normally be close to $\hat{p}$ and thus it represents a *deviated* version of p. On the other hand, $\hat{p}_b$ is a new or *extraneous* pole. Likewise, $\hat{p}*$ is mapped to $\hat{p}*_a$ and $\hat{p}*_b$ which are the complex conjugates of $\hat{p}_a$ and $\hat{p}_b$, respectively. Note that the deviated poles, $\hat{p}_a$ and $\hat{p}*_a$, have higher Q's than the original poles, $\hat{p}$ and $\hat{p}*$. This higher Q-factor increases the peaking at the passband edge of the tunable filter. According to (6), there are two possible mappings for a single pole on the real axis. If the initial pole is greater than $-\rho/4$, it is mapped to a pair of poles on the real axis as shown in Fig. 2(b). Otherwise, the pole is mapped to a pair of complex conjugate poles on the dashed line at $-\rho/2$, as shown in Fig. 2(c).

Since there is no control over the nondominant pole, ρ, the actual mappings in Fig. 2 cannot be predicted or controlled. The tuning system is designed to tune $\hat{p}$, but it actually adjusts the pair of dependent poles $\hat{p}_a$ and $\hat{p}_b$. Thus, although $\hat{p}$ is tuned, the actual response is due to the mapped poles: $\hat{p}_a$ and $\hat{p}_b$. Furthermore, should the nondominant poles of the integrators, ρ, be large in comparison to the frequencies of interest, it can be shown that the deviated poles, $\hat{p}_a$, approach the initial pole, $\hat{p}$, and the extraneous poles, $\hat{p}_b$, would be far enough to the left so that their effects are insignificant. However, with high-frequency filters, the nondominant pole is not large in relation to the pole frequencies of the filter so that the effects of the extraneous poles, $\hat{p}_b$, cannot be ignored. Finally, although Fig. 2 illustrates the mapping of possible pole locations, the mapping of zeros is identical.

The second nonideal effect that is considered is that of the finite dc gain of the integrator, A_0. With finite dc gain, the transfer function of the integrator is still first order but its dominant pole is no longer at dc but at $-1/A_0$. This shift in the dominant pole causes each pole (and zero) of the tunable filter to be shifted to the left. The adaptive approach completely accounts for the finite dc gains of the integrators [9] because it tunes both the poles and zeros. However, finite dc gain is still considered in our investigation as it can be a serious problem for other tuning methods.

The transfer function of an integrator with finite dc gain and no nondominant poles may be expressed as

$$T_{\text{int}}(s) = \frac{1}{s + \frac{1}{A_0}}. \tag{8}$$

Following the method used in (4) through (6), s is replaced by $(s + (1/A_0))$ so that each pole (and zero) of the tunable filter gets shifted as follows:

$$s + \frac{1}{A_0} = \hat{\sigma} + j\hat{\omega}$$

$$s = \hat{\sigma} + j\hat{\omega} - \frac{1}{A_0}. \tag{9}$$

Combining the nonidealities of finite dc gain, A_0, and one nondominant pole, ρ, results in the integrator having the transfer function

$$T_{\text{int}}(s) = \frac{1}{\left(s + \frac{1}{A_0}\right)\left(\frac{s}{\rho} + 1\right)}. \tag{10}$$

The effects of both the finite dc gain and the nondominant pole are illustrated in Fig. 1(c). The finite dc gain causes each pole (and zero) of an ideal Nth-order tunable filter ((3)) to be shifted to the left ((9)), and the nondominant pole causes each pole (and zero) to be mapped to a pair of dependent poles (and zeros) ((6)). This corresponds to each pole (and zero) of (3) being mapped to

$$\left(s + \frac{1}{A_0}\right)\left(\frac{s}{\rho} + 1\right) = \hat{\sigma} + j\hat{\omega} \tag{11}$$

which results in

$$s = -\frac{\rho}{2} - \frac{1}{2A_0} \pm \frac{\rho}{2}\sqrt{\left(1 + \frac{1}{A_0\rho}\right)^2 + \frac{4}{\rho}\left(-\frac{1}{A_0} + \hat{\sigma} + j\hat{\omega}\right)} \tag{12}$$

so that the transfer-function of the tunable filter is $2N$th-order. The $2N$th-order transfer-function may be described by (7), but now the pairs of dependent poles, $\hat{p}_{ia}$ and $\hat{p}_{ib}$, and zeros, $\hat{z}_{ia}$ and $\hat{z}_{ib}$, refer to the mapping defined by (12). Fig. 2 still represents possible pole (or zero) mapping but the mapped poles, $\hat{p}_a$ and $\hat{p}_b$, are now slightly shifted since the finite dc gain, A_0, is included. For example, the dashed line now occurs at $-\rho/2 - (1/2A_0)$. Notice that the phase lead caused by the finite dc gain does partially compensate for the phase lag caused by the nondominant pole. Referring to Fig. 2, the finite dc gain results in the deviated pole, $\hat{p}_a$, being shifted closer to the desired location, $\hat{p}$, so that the peaking at the passband edge is reduced. However, for high-frequency applications, the extraneous pole $\hat{p}_b$ is still close enough to the frequencies of interest so that its effects are still significant.

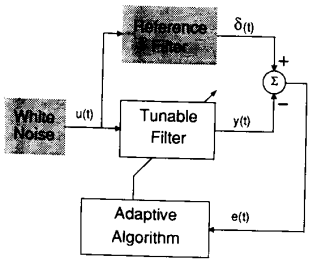

Fig. 3. Adaptive tuning system.

III. The Adaptive Tuning System

The adaptive tuning system is based on the adaptive filter model-matching configuration shown in Fig. 3 [9]. It has been shown that the ideal reference filter is not required if a pseudorandom noise signal is used instead of $u(t)$ and a precalculated reference signal replaces $\delta(t)$. For simplicity, however, the system shown in Fig. 3 is used in the simulations presented in the following sections.

The tunable filter may be realized by any structure that allows the poles and zeros to be varied. In this paper we have chosen to use an implementation based on the adjoint of an orthonormal ladder filter, described in [12]. For an ideal Nth-order transfer-function, N arbitrary poles and zeros may be obtained by adjusting $2N + 1$ coefficients. Since it is assumed that there is at least one zero at infinity, one of these coefficients is set to zero. For the nonideal filter, the specified zero at infinity gets mapped to a pair of dependent zeros at infinity so that the remaining $2N$ variables determine $2N$ poles and $2(N-1)$ zeros. The adaptive algorithm used to adjust the coefficients is a least mean square (LMS) algorithm which minimizes the mean square error (MSE) value of the error signal, $e(t)$. It is important to notice that the adaptive algorithm performs impulse response matching to minimize the MSE value of $e(t)$. Consequently, both magnitude and phase responses are matched. Also, since there is typically more power in the passband of a filter, the adaptive algorithm places more emphasis on tuning the passband (and hence the poles) for a white noise input. Thus, it is expected that there should be better passband than stopband matching. Finally, dc offsets appear to be the most critical problem with the adaptive tuning method. This problem can be corrected by a median-based offset cancellation technique described in [13].

IV. Comparison Between Tuning Only Poles and Tuning Both Poles and Zeros

The first example compares the performance of the popular tuning approach where only the poles are tuned [1]–[8], and the adaptive method where both the poles and zeros are tuned [9]. The desired filter is specified to have a fifth-order transfer-function with a 0.1 dB equiripple passband extending from 0 to 1 rad/s. The desired poles and zeros are:

$$\text{poles: } -0.1581 \pm j1.0785,$$
$$-0.4347 \pm j0.6830, \text{ and } -0.5531$$
$$\text{zeros: } 0 \pm j3.2059, \text{ and three at } \infty.$$

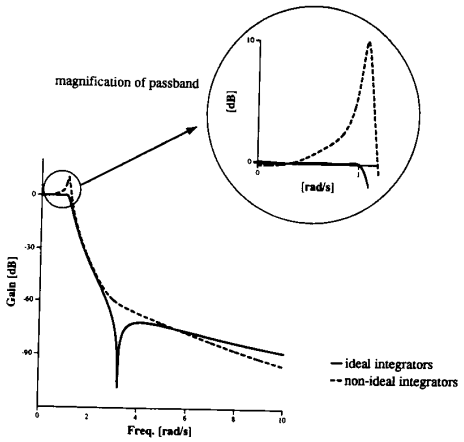

Fig. 4. Transfer-functions of the ideal filter and the filter with nonideal integrators.

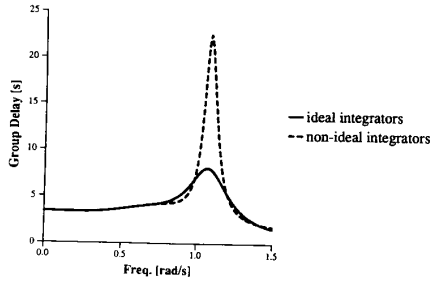

Fig. 5. Group-delay response of the ideal filter and the filter with nonideal integrators.

The solid curves in Figs. 4 and 5 depict the desired transfer-function and group delay response, respectively.

The integrators of the tunable filter are modelled to have finite dc gain and a single nondominant pole as defined in (10). It is assumed that the finite dc gain of the integrator is 100. This is equivalent to having 0.5° phase lead at the unity-gain frequency of the integrator. As this phase lead does partially compensate for the phase lag caused by the nondominant pole of the integrator, the nondominant pole was placed at ten times the passband edge of the desired transfer function so that its effects are still damaging. The nondominant pole at ten times the passband edge corresponds to the integrator having approximately 5° excess phase at the unity-gain frequency of the integrator.

Including finite dc gain and a nondominant pole in each integrator results in a tenth-order transfer-function, shown by the dashed curves in Figs. 4 and 5. Fig. 6 shows a pole-zero plot of the ideal filter and the filter with nonideal integrators. Each pole is mapped to two poles: five deviated poles, which are close to the desired pole locations, and five extraneous poles on the left. The peaking at the passband edge in Fig. 4 arises from the higher Q-factor of the deviated poles. The five extraneous poles do not correspond to any desired poles and must therefore be cancelled for exact matching. The finite zeros on the $j\omega$ axis are mapped to two pairs of dependent

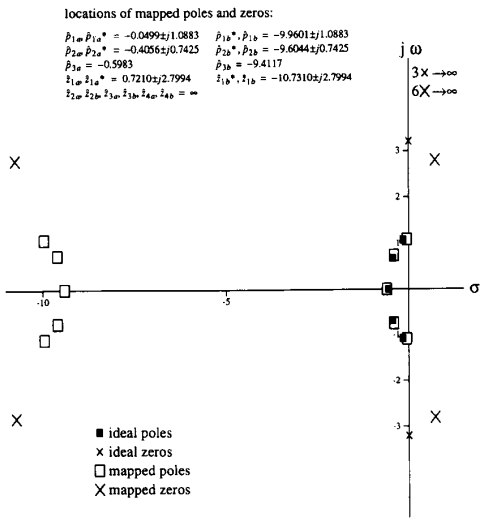

Fig. 6. Ideal and mapped poles and zeros.

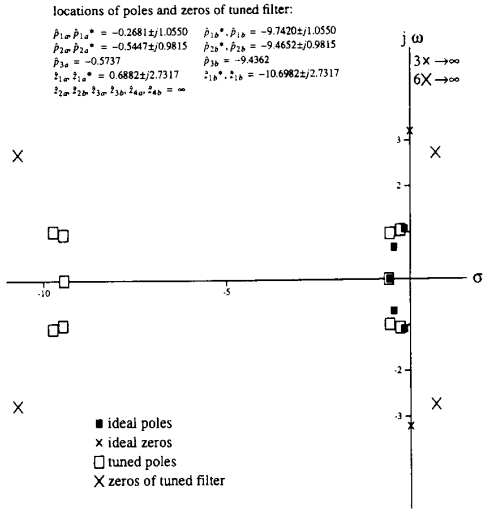

Fig. 7. Pole-zero plot when only the poles are tuned.

zeros $(\hat{z}_{1a}, \hat{z}_{1b})$ and $(\hat{z}*_{1a}, \hat{z}*_{1b})$, none of which is on the $j\omega$ axis and thus the notch is lost. The zeros at $\hat{z}_{1b}$ and $\hat{z}*_{1b}$ do partially cancel the effects of the five extraneous poles but this is clearly not enough to completely eliminate their effects. Finally, instead of three zeros at infinity, the nonideal system has six zeros at infinity which results in excess stopband attenuation.

The first simulation restricts the adaptive algorithm to only vary the poles of the filter. Specifically, the poles of the adjoint of the orthonormal ladder structure are tuned by varying N parameters in the circuit realization. Although this affects the finite zeros of the filter, the effect is no different than that encountered in the master-slave approach where the zero locations are affected by the changes made in the poles' ω_0 and Q. Note that although zeros may change when poles are tuned with the master-slave method, the zeros do not necessarily change in an optimum fashion from the point of view of minimizing the effects of parasitics, as the zeros are not directly adjusted.

Fig. 7 shows the pole and zero locations of the tuned filter, and the dashed curves in Figs. 8 and 9 illustrate its frequency response. The results confirm that both passband and stopband are not exactly matched to the desired transfer-function as tuning only poles simply does not give enough degrees of freedom. As illustrated in Fig. 8, the passband peak is reduced, as the deviated poles are moved to the left, but the ripple certainly does not meet the given specifications. As well, the effects of the extraneous poles on the left cannot be eliminated by just adjusting the poles. These extraneous poles cannot be cancelled as zeros are not tuned, and they cannot be pushed away as they are dependent on the deviated poles which the adaptive algorithm uses to match the response of the desired poles. Furthermore, the excess zeros at infinity still give too much attenuation at high frequencies and the notch is not matched as zeros are not directly varied. This suggests that tuning the zeros is necessary to better match the desired

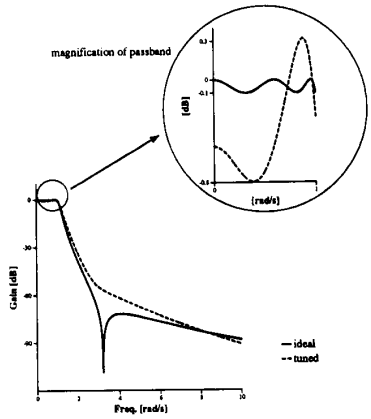

Fig. 8. Magnitude response when only the poles are tuned.

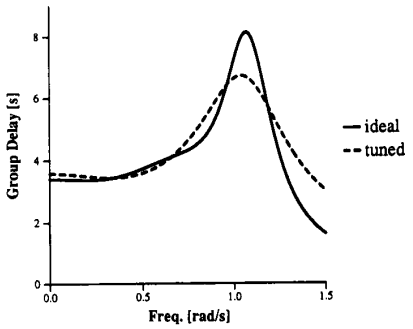

Fig. 9. Group-delay response when only the poles are tuned.

transfer-function by matching the desired zeros and cancelling the effects of the extraneous poles.

The second simulation allows the tuning of both the poles and zeros. The locations of the tuned poles and zeros are

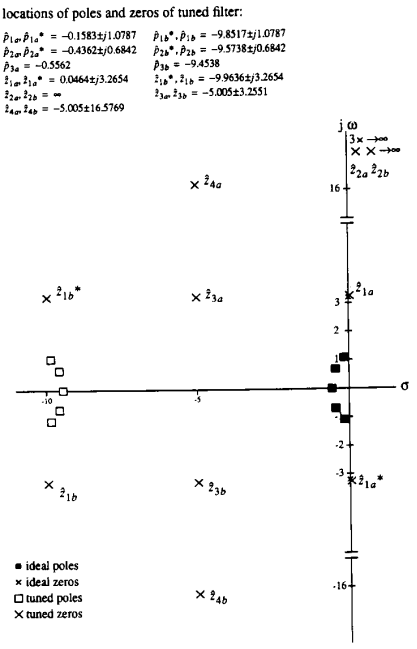

Fig. 10. Pole-zero plot when both poles and zeros are tuned.

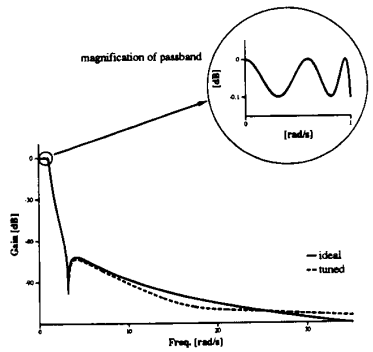

Fig. 11. Magnitude response when both poles and zeros are tuned.

shown in Fig. 10, and the tuned transfer-function and group-delay response are represented by the dashed curves in Figs. 11 and 12, respectively. Although the ideal and tuned passbands are not identical, the magnification in Fig. 11 shows that the responses are nearly indistinguishable. Also, the notch is accurately tuned. Since the adaptive algorithm places more emphasis on tuning the passband, consider the poles first. Fig. 10 shows that the five deviated poles are tuned to match the desired pole locations. As in the previous case, the effects of the five extraneous poles on the left must be cancelled for accurate matching. However, unlike the previous case, the tuning of zeros does allow more degrees of freedom to cancel the effects of these extraneous poles.

When adjusting the zeros, the adaptive algorithm must place the zeros to match the five desired zeros as well as to cancel the effects of the extraneous poles. The finite pair of complex

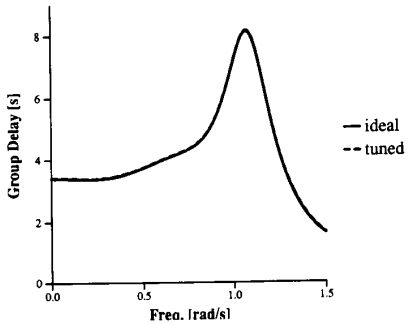

Fig. 12. Group-delay response when both poles and zeros are tuned.

conjugate zeros is matched rather accurately with $\hat{z}_{1a}$ and $\hat{z}*_{1a}$. As seen in Fig. 10, the resulting extraneous zeros, $\hat{z}_{1b}$ and $\hat{z}*_{1b}$, do give some cancellation of the poles on the left but more cancellation is necessary. Now consider the remaining three pairs of dependent zeros which, according to Fig. 6, are initially at infinity. As stated before, the tunable filter is forced to have at least one pair of dependent zeros at infinity. This accounts for two of the three desired zeros at infinity. Thus, instead of using two pairs of dependent zeros, $(\hat{z}_{2a}, \hat{z}_{2b})$ and $(\hat{z}_{3a}, \hat{z}_{3b})$, to match two zeros at infinity, only one pair of dependent zeros, $(\hat{z}_{2a}, \hat{z}_{2b})$, is used. Consequently, the adaptive algorithm has a *free* pair of dependent zeros $(\hat{z}_{3a}, \hat{z}_{3b})$ to be used for the sole purpose of cancelling the effects of the extraneous poles. This pair is referred to as *free* because it is not required to match any desired zeros. As shown by the possible pole mappings in Fig. 2 and using (12), this pair of dependent zeros is restricted to vary along the $-p/2-(1/2A_0)$ dashed line or along the real axis. Fig. 10 shows that the free zeros are tuned to $-5.005 \pm j3.2551$ to further cancel the extraneous poles. Finally, matching the third desired zero at infinity is compromised as $\hat{z}_{4a}$ and $\hat{z}_{4b}$ are pulled away from infinity and placed on the -5.005 line. The result is a mildly insufficient attenuation at high frequencies.

In summary, it is evident that better results are achieved when the poles and zeros are tuned. Because the nonideal integrators affect both the poles and zeros, the initial zero locations are corrupted and must be adjusted. Tuning systems which vary only the poles cannot account for incorrect zeros and thus do not give good results. Furthermore, it was seen that the tuning of zeros enables the reduction of the effects of the extraneous poles, though at the expense of not matching all the zeros. A special benefit is also seen when a free pair of tunable zeros is obtained from using a pair of dependent zeros to match two zeros at infinity. Therefore, in choosing a transfer-function, it is better to have at least one pair of zeros at infinity. The importance of tuning zeros is also seen when tuning all-pole filters such as a fifth-order Chebyshev filter. Simulation results show that the passband is accurately matched by moving zeros at infinity to finite locations to partially compensate extraneous poles. This would not occur with a master-slave approach as both desired and extraneous zeros remain at infinity. However, for the sake of brevity, these results were not included.

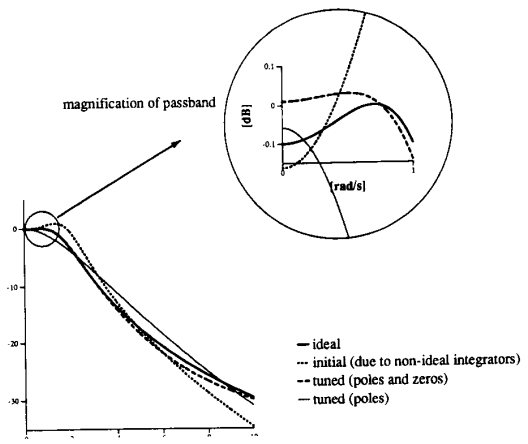

Fig. 13. Magnitude response of biquad example.

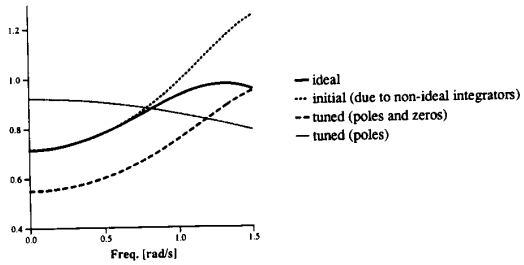

Fig. 14. Group delay response of biquad example.

V. Biquad Example

A common approach of applying tuning methods is to realize the continuous-time filter by a cascade of biquads and tune each biquad section individually [1]–[8]. Hence, using integrators modelled by the nonidealities discussed in Section II, results from the adaptive tuning system and a master–slave approach are compared here. The master–slave approach is emulated by impulse response matching where the pole frequency, quality factor, and dc gain are all adjusted.

The poles and zeros of the desired transfer-function are

$$\text{poles: } -1.1862 \pm j1.3810$$

$$\text{zeros: } \infty, \infty.$$

Figs. 13 and 14 respectively show the transfer-functions and group delay responses of the ideal, initial, and tuned filters. As before, the initial transfer-function represents the transfer function that arises from having nonideal integrators. First consider the results when only the poles and dc gain are tuned. Notice that the ripple in the passband is much greater than 0.1 dB and that there is still too much stopband attenuation as the zeros at infinity are not adjusted. On the other hand, better matching is obtained when both poles and zeros are tuned. The peak at the passband edge has been reduced but there is still some discrepancy between the tuned and ideal transfer-functions. Finally, note that the group delay responses of both tuned filters are not accurate. Thus the results show that tuning only the poles and dc gain give worse results than tuning both poles and zeros, even in the second-order case.

Although the adaptive tuning system does give better tuning results than just tuning the poles and dc gain, the adaptive method does not accurately tune the biquad as in the fifth-order example. This occurs as a biquad does not have enough degrees of freedom to cancel the parasitic effects. Fig. 15 depicts the ideal pole and zero locations as well as the pole and zero locations of the filter in which both the poles and zeros are tuned. As expected, the pair of deviated poles, $\hat{p}_{1a}$ and $\hat{p}*_{1a}$, is placed close to the desired pair of poles. Each of

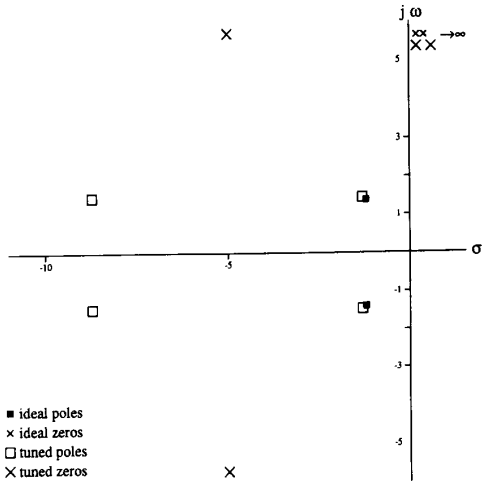

Fig. 15. Pole-zero plot when both poles and zeros are tuned for biquad example.

the poles, $\hat{p}_{1a}$ and $\hat{p}*_{1a}$, has a dependent pole to the left so that there is a complex conjugate pair of extraneous poles, $\hat{p}_{1b}$ and $\hat{p}*_{1b}$, which must be cancelled by zeros. The adaptive algorithm has two pairs of dependent zeros to match two desired zeros at infinity and to attempt to cancel the effects of the extraneous poles. Specifically, a pair of dependent zeros is automatically placed at infinity thus giving a free pair of dependent zeros to be used for cancelling the extraneous poles. However, as shown in Fig. 2, this pair of dependent zeros is restricted to vary along the $-p/2 - (1/2A_0)$ dashed line or along the real axis. Fig. 15 shows that the free zeros are tuned to $-5.005 \pm j5.6997$. Obviously this does not completely cancel the extraneous poles, $\hat{p}_{1b}$ and $\hat{p}*_{1b}$, so the final values for the poles $\hat{p}_{1a}$ and $\hat{p}*_{1a}$ do not match the desired poles exactly.

The results show that there are not enough degrees of freedom to exactly tune a biquad to an ideal transfer-function. As shown in Fig. 13, adaptive tuning does reduce the parasitic effects; however, the passband is not as accurately tuned as the fifth-order example discussed in the previous section. The fifth-order transfer-function gives more opportunities for the

adaptive algorithm to reduce the parasitic effects of the extraneous poles by trading-off exact zero matching. Therefore, higher order transfer-functions give more degrees of freedom for tuning and thus have better results.

VI. Conclusions

This paper investigated the problems that arise in tuning filters constructed using integrators with finite dc gain and a single nondominant pole. The finite dc gain does not increase the order of the tunable filter but shifts each pole and zero to the left. Since the adaptive algorithm tunes *both* poles and zeros, it has no problem dealing with shifts in the poles and zeros. On the other hand, the single nondominant pole in each integrator doubles the order of the tunable filter, by mapping each pole and zero to a pair of dependent poles and zeros, respectively, but does not increase the number of elements that may be independently varied for tuning purposes. This is a serious problem that becomes particularly harmful for high-frequency filters.

Simulation results show that the adaptive tuning system is superior to methods that tune only the poles of the filter. Zero tuning not only corrects for erroneous zero locations but also allows trade-off between exact zero matching and the placing of the zeros such as to partially cancel the effects of the extraneous poles to achieve better overall passband performance. The results also indicate that the type of transfer-function chosen to meet specifications influences how accurately the filter is tuned. Specifically, as shown by the results of the fifth-order and biquad examples, there are more degrees of freedom for tuning with higher order filters. It was also shown that using a pair of dependent zeros to match a pair of desired zeros at infinity gives a free pair of dependent zeros to be used for cancelling the effects of the extraneous poles. This all suggests a fruitful area of researchfinding the best filter transfer-function from a tunability point of view.

References

[1] R. Schaumann, M. S. Ghausi, and K. R. Laker, *Design of Analog Filters: Passive, Active RC, and Switched Capacitor.* Englewood Cliffs, NJ: Prentice-Hall, 1990.

[2] V. Gopinathan, Y. P. Tsividis, K. S. Tan, and R. K. Hester, "Design considerations for high-frequency continuous-time filters and implementation of an antialiasing filter for digital video," *IEEE J. Solid-State Circuits*, vol. 25, pp. 1368–1378, Dec. 1990.

[3] R. Schaumann and M. A. Tan, "The problem of on-chip automatic tuning in continuous-time integrated filters," *Proc. 1989 IEEE Int. Symp. Circuits and Systems*, pp. 106–109, Feb. 1989.

[4] C. S. Park and R. Schaumann, "Design of a 4 MHz analog integrated CMOS transconductance-C bandpass filter," *IEEE J. Solid-State Circuits*, vol. 23, pp. 987–996.

[5] F. Krummenacher and N. Joehl, "A 4-MHz CMOS continuous-time filter with on-chip automatic tuning," *IEEE J. Solid-State Circuits*, vol. 23, pp. 750–758, June 1988.

[6] H. Khorramabadi and P. R. Gray, "High-frequency CMOS continuous-time filters," *IEEE J. Solid-State Circuits*, vol. 19, pp. 939–948, Dec. 1984.

[7] Y. P. Tsividis, M. Banu, and J. Khoury, "Continuous-time MOSFET-C filters in VLSI," *IEEE J. Solid-State Circuits*, vol. 21, pp. 15–30, Feb. 1986.

[8] C.-F. Chiou and R. Schaumann, "Design and performance of a fully integrated bipolar 10.7 MHz analog bandpass filter," in *IEEE Trans. Circuits Syst.*, vol. 33, pp. 116–124, Feb. 1986.

[9] K. A. Kozma, D. A. Johns, and A. S. Sedra, "Automatic tuning of continuous-time integrated filters using an adaptive filter technique," *IEEE Trans. Circuits Syst.*, vol. 38, pp. 1241–1248, Nov. 1991.

[10] C. G. Yu, W. G. Bliss, and R. L. Geiger, "A tuning algorithm for digitally programmable continuous-time filters," in *Proc. 1991 IEEE Int. Symp. Circuits and Systems*, pp. 1436–1439, June 1991.

[11] A. S. Sedra and K. C. Smith, *Microelectronic Circuits*, third ed. Philadelphia, PA: Saunders College Publishing, 1991.

[12] D. A. Johns, W. M. Snelgrove, and A. S. Sedra, "Orthonormal ladder filters," *IEEE Trans. Circuits Syst.*, vol. 36, pp. 337–343, Mar. 1989.

[13] A. S. Shoval, D. A. Johns, and W. M. Snelgrove, "Median-based offset cancellation circuit technique," in *Proc. 1992 IEEE Int. Symp. Circuits and Systems*, pp. 2033–2036, May 1992.

Karen A. Kozma (S'88) received the B.A.Sc. and the M.A.Sc. degrees in electrical engineering from the University of Toronto in 1988 and 1990, respectively.

She is currently working towards the Ph.D. degree at the same university in the area of high-frequency continuous-time filters.

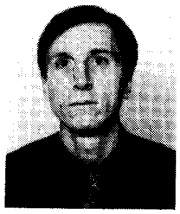

David A. Johns received the B.A.Sc., M.A.Sc. and Ph.D. degrees from the University of Toronto, Canada, in 1980, 1983, and 1989, respectively.

From 1980 to 1981 he worked as an applications engineer in the semiconductor division of Mitel Corp., Ottawa, Canada. From 1983 to 1985 he was an analog IC designer at Pacific Microcircuits Ltd., Vancouver, Canada. Upon completion of his doctoral work, he was hired at the University of Toronto, where he is currently an Assistant Professor. His research interests are in the areas of integrated circuit design and signal processing.

Adel Sedra received the B.Sc. degree from Cairo University, Egypt, in 1964, and the M.A.Sc. and Ph.D. degrees from the University of Toronto, Canada, in 1968 and 1969, respectively, all in electrical engineering.

From 1964 to 1966, he served as Instructor and Research Engineer at Cairo University. Since 1969 he has been on the staff of the University of Toronto where he is currently Professor and Chairman of the Department of Electrical Engineering. He has also served as a consultant to industry and government in Canada and the United States; he was President of Electrical Engineering Consociates Ltd., a research and design consulting company, from 1979 to 1981; he was the founding Executive Director of the University of Toronto Microelectronics Development Centre from 1983 to 1986; and he was a founding member and serves on the board of the Information Technology Research Centre, a designated center-of-excellence funded by the Province of Ontario. He specializes in the area of microelectronics. His research has centered on the theory and design of circuits for communication and instrumentation systems and has resulted in about 120. Two papers, co-authored with his graduate students, were selected by the IEEE to receive awards\colon the 1984 Darlington Award and the 1986 Guillemin-Cauer Award. He has co-authored two textbooks: *Filter Theory and Design* (1978) and *Microelectronic Circuits* (1982; 1987; and third edition 1991).

In 1988, Dr. Sedra was the recipient of the Frederick Emmons Terman Award, given by the American Society for Engineering Education. He has served the Circuits and Systems Society of the IEEE in a variety of administrative and editorial positions, and is a registered professional engineer in the province of Ontario.